Published in final edited form as:
Neuroscience. 2010 February 3; 165(3): 715. doi:10.1016/j.neuroscience.2009.11.003.

Monitoring transient Ca^{2+} dynamics with BK channels at active zones in frog saccular hair cells

Thanh Sy[1], **Alan D. Grinnell**[2], **Arthur Peskoff**[2], and **Bruce Yazejian**[1]

[1] Department of Biology, Mount St. Mary's College, Los Angeles, CA 90049

[2] Department of Physiology, David Geffen School of Medicine, UCLA, Los Angeles, CA 90095

Abstract

Neurotransmitter release from the basolateral surface of auditory and vestibular hair cells is mediated by Ca^{2+} influx through voltage-gated Ca^{2+} channels. Co-localization of large-conductance Ca^{2+}-activated K^+ (BK) channels at the active zones of these cells affords them with an optimal location to act as reporters of the Ca^{2+} concentration changes at active zones of transmitter release. In this report we use BK channels to monitor dynamic changes in intracellular Ca^{2+} concentration during transient influxes of Ca^{2+}, showing that BK current magnitude and delay to onset are correlated with the rate and duration of Ca^{2+} entry through Ca^{2+} channels. We also show that BK channels exhibit a much higher Ca^{2+} binding affinity in the open state than in the closed state.

Keywords

patch clamp; Ca^{2+} channels; transmitter release

Introduction

The release of neurotransmitter is triggered by a rapid rise in the intracellular free Ca^{2+} concentration due to the influx of Ca^{2+} through nerve terminal voltage gated Ca^{2+} channels opened by depolarization (Katz, 1969; Augustine et. al., 1987; Clapham, 2007). The spatial and temporal restriction of Ca^{2+} to active zones—regions near Ca^{2+} channels that are the sites of transmitter release—is achieved through the action of low affinity Ca^{2+} buffers with rapid kinetics (Zucker, 1996; Neher, 1998; Roberts, 1993, 1994; Issa and Hudspeth, 1996). Perhaps equally important—to enable repetitive signaling—is the subsequent rapid reduction of the active zone Ca^{2+} concentration to baseline levels following closure of the Ca^{2+} channels. Rapid build-up and decay of concentrations of Ca^{2+} high enough to trigger transmitter release are especially important for auditory and vestibular hair cells that can release transmitter at very high frequencies (Smotherman and Narins, 1999; Fettiplace and Fuchs, 1999; Glowatzki and Fuchs, 2002; Fuchs, 2005; Rutherford and Roberts, 2009). In order to track the time course of the changes in intracellular Ca^{2+} concentration at active zones we monitored the activity of large-conductance Ca^{2+}-dependent K^+ (BK) channels in frog saccular hair cells that co-localize at active zones with Ca^{2+} channels (Roberts, et. al., 1990; Issa and Hudspeth, 1994; Armstrong

Address for correspondence: Bruce Yazejian, Department of Biology, Mount St. Mary's, College, 12001 Chalon Road, Los Angeles, CA 90049; Phone: (310) 954-4105; FAX: (310) 954-4052; byazejian@msmc.la.edu.

Section Editor: Dr. Menahem Segal, Weizmann Institute of Science, Department of Neurobiology, Hertzl Street, Rehovot 76100, Israel

and Roberts, 1998, 2001). Ca^{2+}-activated channels have previously been used to estimate the intracellular Ca^{2+} concentration in a number of preparations (Roberts et al., 1990; Tucker and Fettiplace, 1996; Prakriya and Lingle, 2000; Yazejian et al., 2000). In this report we use BK channels to track intracellular Ca^{2+} concentration changes that result from transient fluxes of Ca^{2+} through Ca^{2+} channels. We show that the time to onset and extent of activation of BK channels depend upon the rate and duration of Ca^{2+} entry. The slow rate of BK channel deactivation—at depolarized voltages where Ca^{2+} influx is terminated—reflects either the intrinsic kinetics of BK channel closure or the much greater Ca^{2+} binding affinity of channels in the open state.

Experimental procedures

Cell isolation

All animals used in this study were handled in compliance with the policies and procedures of the Animal Care and Use Committee at Mt. St. Mary's College and with the National Institute of Health Guide for the Care and Use of Laboratory Animals (NIH Publications No. 80–23). Hair cells were isolated from the sacculus of the grass frog (*Rana pipiens*) as described previously (Hudspeth and Lewis, 1988). Sacculi were dissected free from the labyrinth and immersed in a low Ca^{2+} solution (LoCaS) of the following composition: 100 mM NaCl, 2 mM KCl, 50 μM $CaCl_2$, 50 μM $MgCl_2$, 3 mM glucose, 30 mM HEPES, pH 7.3, supplemented with cysteine-activated papain (0.5 mg/ml L-cysteine + 0.5 mg/ml papain (Calbiochem 5125)). After 30–60 minutes in papain, sacculi were moved to fresh LoCaS supplemented with 1 mg/ml BSA for 60 minutes. Sacculi were then transferred to a recording dish containing frog Ringer of the following composition: 116 mM NaCl, 2 mM KCl, 1 mM $CaCl_2$, 1 mM 3,4 diaminopyridine (DAP) and 5 mM HEPES, pH 7.3. The Ringer solution was supplemented with 10 nM of the specific BK channel blocker paxilline (Sanchez and McManus, 1996). This was done to reduce the magnitude of the BK currents to allow for adequate voltage control. A dog hair (Weimaraner) was used to scrape off the cells from the epithelium.

Electrophysiology

Patch electrodes were fabricated from borosilicate glass (Sutter BF 150-86) using a two-stage puller (Narishige PP-97) to yield tip diameters of about 1 μm with an electrode resistance (with our internal solutions, see below) of 3–5 MΩ. To record BK currents, pipettes were filled with a quasi-internal solution of the following composition: 52 mM K_2SO_4, 38 mM KCl, 1 mM K-EGTA, 1 mM DAP and 5 mM HEPES pH 7.3, supplemented with 200–300 μg/ml amphotericin-B. To record Ca^{2+} currents, the pipettes were filled with a solution of the following composition: 52 mM $CsMeSO_4$, 38 mM CsCl, 1 mM EGTA, 1 mM DAP, 50 mM D-glucose, 5 mM HEPES, pH 7.3 and amphotericin-B as above. For Ca^{2+} current recordings the bath solution was switched to one of the following composition: 116 mM NaCl, 2 mM KCl, 2 mM $CaCl_2$, 10 mM TEACl, 1 mM 3,4 diaminopyridine (DAP), 1 μM paxilline and 5 mM HEPES, pH 7.3. Perforated patch recordings (Horn and Marty, 1988; Rae et al., 1991) were performed using a MultiClamp 700B patch-clamp amplifier in combination with a Digidata 1440A analog-to-digital interface (Molecular Dynamics, Foster City, CA). Pulse paradigms and data analysis were performed with the pCLAMP 10 suite of software programs (Molecular Dynamics). Currents were acquired at 50 kHz and filtered at 10 kHz. Series resistance (typically 8–15 M Ω) was compensated 85–95% and linear leak and capacitive currents were subtracted using a P/-8 protocol (Bezanilla and Armstrong, 1977). Experiments were performed at room temperature (22–24°C). Figures were made with the Origin 7.5 graphing software package (Microcal).

Results

BK channel activation with different rates and durations of Ca^{2+} entry

Figure 1 shows results from an experiment designed to monitor the build-up and decay of intracellular Ca^{2+} as a function of the rate and duration of Ca^{2+} entry using BK currents as a measure of submembrane [Ca^{2+}]. Voltage pulse paradigms are shown above each set of records with the intermediate potentials (IPs) indicated (see below). For these experiments the membrane voltage was initially stepped from a holding potential of −70 mV to +130 mV (above the Ca^{2+} equilibrium potential) for 10 msec to maximize the opening of voltage-gated Ca^{2+} channels while minimizing the Ca^{2+} driving force. Thus, at +130 mV a maximum number of Ca^{2+} channels opened but no Ca^{2+} influx occurred. After this initial step, the voltage was repolarized to IPs of +130 mV (*i.e.* no step change), +50 mV, +10 mV, −30 mV or −70 mV for durations of 100 μsec, 300 μsec, 500 μsec, 1 msec, 3 msec and 5 msec before returning to +130 mV for an additional 80 msec.

During the IP steps Ca^{2+} entry occurred independent of Ca^{2+} channel opening kinetics (Hudspeth and Lewis, 1988) and continued as long as the Ca^{2+} channels remained open. Furthermore, the rate of Ca^{2+} entry was dependent on the Ca^{2+} driving force at each IP. The IP steps generated a mixed current of Ca^{2+} flowing through already opened Ca^{2+} channels and BK channel current flowing in response to the rise in the free Ca^{2+} concentration resulting from the Ca^{2+} influx. Subsequent re-depolarizations to +130 mV then generated currents that largely flowed through BK channels as Ca^{2+} entry was terminated and the driving force for BK channel current was increased. Thus, the evoked BK currents measured during the second step to +130 mV should reflect the [Ca^{2+}] present near the BK channels just prior to and during the step depolarization. For very short duration IPs, where few BK channels have opened, the subsequent step to +130 mV generated a BK current flowing mostly through channels that opened due to this step change of voltage, but were not open during the IP. On the other hand, after longer times spent at the IP the BK current seen at +130 mV predominately flowed through channels that had opened at the IP and were suddenly subjected to a larger K^+ driving force. As the BK channels might be expected to close at a rate consistent with the decline of the free Ca^{2+} concentration, the duration of the BK current at +130 mV (where Ca^{2+} influx ceases) may potentially be a measure of the duration of a concentration of free Ca^{2+} sufficient to maintain BK channel opening.

Figure 1A shows that, superimposed on a Ca^{2+}-independent outward current in response to the initial +130 mV step, a 100 μsec IP step to either −70 mV or −30 mV led to the generation of an additional outward current during the second step to +130 mV (solid black and green traces respectively). As these outward currents occurred only after the IP steps (compare with the dotted line showing the current in response to a step to +130 mV only), they are consistent with their being BK currents flowing in response to the Ca^{2+} influx during the IP. In fact, these outward currents were blocked by application of 100 nM of the BK channel blocker paxilline (Sanchez and McManus, 1996) (see inset a of Figure 1). At an IP duration of 100 μsec, the largest BK current evoked at +130 mV was seen in response to the IP of −70 mV. With longer durations at the IP of −70 mV the magnitude of the BK current generated during the second +130 mV step increased, reached a maximum with an IP step duration of 300 μsec, and then declined in peak magnitude as the potential was held at this IP for longer and longer times (compare the black traces in Figure 1 A-F). By comparison, at an IP step of +50 mV (red traces) there was no BK current generated during the +130 mV step that followed the 100 μsec IP step (red trace in Figure 1A) and only a very small current was seen with a 300 μsec step (when the step to −70 mV yielded the largest current for that IP). However, longer durations at +50 mV led to larger and larger BK currents, becoming maximal at 5 msec IP duration (Figure 1F).

At −70 mV, where the Ca^{2+} driving force would be the greatest, one would expect the greatest rate of Ca^{2+} entry. On the other hand, at this potential Ca^{2+} channels close rapidly leading to a decline in the Ca^{2+} influx and a limit to the free Ca^{2+} concentration near the BK channels. In contrast, at +50 mV one would expect a slower but continuous Ca^{2+} influx due to the lower Ca^{2+} driving force and maintained channel opening. These features of the expected Ca^{2+} influx are observed with the BK current behavior as measured at +130 mV. That is, for the IP of −70 mV, the BK current turned on with short durations of Ca^{2+} entry (*e.g.* the first 100 μsec of the tail current) and diminished rapidly as the potential was maintained at −70 mV before stepping to +130 mV. Likewise, the BK current measured at +130 mV in response to the IP step of +50 mV built up slowly but didn't diminish in magnitude for long IP durations (*e.g.* 5 msec).

Figure 2 summarizes results from several experiments like that of Figure 1. Plotted are the normalized BK peak current magnitudes measured at +130 mV as a function of the time spent at different IPs. Note that the *peak magnitudes* of the responses are plotted here and not the time courses of the responses themselves. As was seen in Figure 1, the peak current magnitude measured after the IP steps to −70 mV increased most quickly (requiring the shortest duration of Ca^{2+} entry), and fell most quickly, being back to baseline by 2 msec of IP duration. Similar phasic responses in the magnitude of the BK currents were seen with IPs of −50 mV and −30 mV (and to a lesser extent, −10 mV) but in these cases the maximum BK magnitudes obtained were larger, the peak responses required longer IP durations, and the BK current magnitudes fell more slowly. The BK current magnitude responses to IPs between +10 mV and +50 mV were slower still in reaching their peak values and did not decline for longer IP durations. The plot of the responses to the IP of +70 mV was the slowest of all: even 3 msec of Ca^{2+} entry at this potential was insufficient to activate all of the BK channels that could be activated by the 3 msec steps to IPs between +10 mV and +50 mV.

Correlation of Ca^{2+} currents with BK channel activation

To understand the relationship between the magnitude and rate of Ca^{2+} entry during the IP steps and the subsequent BK currents measured at +130 mV, we recorded Ca^{2+} currents in response to the same waveforms as presented in Figure 1. Figure 3 shows these measured Ca^{2+} currents (continuous traces, inverted for clarity) in response to steps from +130 mV to the IPs of −70 mV, −10 mV and +50 mV. Superimposed on these Ca^{2+} currents are the corresponding normalized BK current magnitudes measured during steps to +130 mV after different durations at these IPs (as in Figure 2).

The Ca^{2+} tail current recorded in response to a step from +130 mV to −70 mV (left panel) peaked in magnitude in less than 300 μsec and was over in less than 1 msec. The BK current magnitude responding to a +130 mV step given at different times during the tail current peaked slightly later than the peak of the Ca^{2+} current and declined with a delay, persisting for about 1 msec after the cessation of the Ca^{2+} influx. The middle panel shows the Ca^{2+} current measured during a step from +130 mV to −10 mV and the BK responses (again, measured at +130 mV) at various times during this IP step. Here the Ca^{2+} current was slower to rise and the peak smaller than at −70 mV, but the influx declined only slightly, persisting throughout the 3 msec step. The BK current magnitudes associated with fractions of this Ca^{2+} current rose more slowly (than the current magnitudes in response to the steps to −70 mV) but reached a larger peak value before declining slightly. Finally, the Ca^{2+} current recorded in response to the step to +50 mV had the slowest rate of rise and the smallest peak value. Unlike the other two, it did not decline after reaching its peak value. The BK currents for this IP also rose in magnitude more slowly but—unlike the responses to −70 mV—and −10 mV steadily increased in response to increasing fractions of the Ca^{2+} influx during the 3 msec step.

The slow influx of Ca^{2+} during the step to +50 mV led to an accumulation of intracellular Ca^{2+} that was able to open as many BK channels as the rapid Ca^{2+} influx at −10 mV but required

more Ca^{2+} influx time. On the other hand, because of the brief influx of Ca^{2+} at −70 mV, only about half as many BK channels were activated as could be activated with IP steps to −10 mV and +50 mV. The correlation of the rate of rise and fall of the magnitude of the BK current in response to different rates and durations of Ca^{2+} entry suggests that BK channels were closely monitoring the Ca^{2+} concentration changes that were occurring during these voltage steps and gives an indication of the speed with which the Ca^{2+} concentration rose above threshold for activation of BK channels.

BK channel deactivation after exposure to high [Ca^{2+}]

The results from Figure 1 suggest that, for each trace, the decline of the BK current during the maintained +130 mV step reflects the rate of disappearance of a Ca^{2+} concentration sufficient to maintain BK channels in an open configuration. This follows from the presumption that, as the potential approaches +130 mV, the Ca^{2+} influx should stop and that any persistent BK channel conductance should be a result of lingering free Ca^{2+} near the BK channels. Note that this decline in the BK current is deactivation, not inactivation. The evidence for this is twofold. First, as reported by Armstrong and Roberts, 1998,2001) the inactivation of BK channels in frog saccular hair cells is removed by papain. Our cell isolation procedure includes this enzyme treatment (see Experimental Procedures). Second, as shown in inset b of Figure 1, the BK current was maintained (*i.e.* did not inactivate) when the test potential given after the IP step was below E_{Ca2+} where Ca^{2+} influx continued. It is unclear however, whether the decline in the BK currents themselves at +130 mV (as opposed to the decline in their maximum elicitable magnitudes) was due primarily to the decline in the ambient [Ca^{2+}] near them or to the kinetics of deactivation of the BK channels.

To distinguish between these possibilities we performed the experiments of Figure 4. Figures 4A and 4B show results from experiments where the membrane potential was stepped to an IP of either +10 mV or −30 mV for 5 msec before testing the BK current response at +130 mV (similar to the experiments illustrated in Figure 1F). However, (unlike the experiments of Figure 1F), after 5 msec at +130 mV, the potential was transiently repolarized to −70 mV for different lengths of time before returning to +130 mV for an additional 80 msec. Stepping to −70 mV should have two effects. First, it should lead to the deactivation of BK channels and second it should close the Ca^{2+} channels and stop the entry of Ca^{2+} (after allowing a transient Ca^{2+} influx from the tail current). Upon return to +130 mV, BK channels should re-open depending on the available Ca^{2+} (including residual Ca^{2+} from the IP step and the additional Ca^{2+} from the tail current).

Consider first the responses to the IP of +10 mV (Figure 4A). The solid black trace indicates the control response to a waveform where the second step to +130 mV was uninterrupted (*i.e.* no step to −70 mV). A short sojourn to −70 mV (0.5 msec—red trace) led to a BK current at +130 mV that reached nearly the same magnitude as the current in the uninterrupted trace and that declined at a similar rate. However, after longer times spent at −70 mV before return to +130 mV (*e.g.* 1 msec-blue trace) the peak BK current evoked was less than the current at that time in the uninterrupted pulse. Evidently the BK channels that closed during the 1 msec step to −70 mV did not reopen upon re-depolarization to +130 mV to the level of the black trace (*i.e.* no step to −70 mV) even though the Ca^{2+} concentration near the BK channels at that time during the +130 mV step was likely to have been no lower than it would have been had the step to −70 mV not been made. In fact there was probably more Ca^{2+} due to the influx of Ca^{2+} during the tail current. Holding the potential at −70 mV for increasingly longer times (greater than 1.5 – 2.0 msec) exceeded the time of the Ca^{2+} tail current (*cf.* Figure 3). As a result, the subsequent steps to +130 mV generated no BK current since after these long sojourns at −70 mV there was evidently not enough Ca^{2+} to re-open them.

Figure 4B shows the results from a similar experiment but where the IP step was to −30 mV instead of +10 mV. Note that—in contrast to the result with a +10 mV IP—the 0.5 msec sojourn to −70 mV after the IP step (red trace) led to a larger BK current at +130mV than was seen without the interruption—likely due to the re-opening of BK channels due to the Ca^{2+} tail current. As with the paradigm with the +10 mV IP step, longer interruptions of the +130 mV step to −70 mV led to rapid closure of the open BK channels that could not be re-opened by the step back to +130 mV. In both cases (the IPs of +10 mV and −30 mV) the BK channels that would have remained open at +130 mV were unable to re-open if they were closed with a prolonged step to −70 mV.

Another set of experiments designed to test the BK channel's ability to track the Ca^{2+} concentration changes at the active zone is illustrated by the results in the bottom panel of Figure 4. In these experiments Ca^{2+} entry was terminated (save for a Ca^{2+} tail current) and BK and Ca^{2+} channels were closed following 5 msec steps to +10 mV or −30 mV by stepping to −70 mV for various times *before* testing the BK channel status at +130 mV. Immediate steps to +130 mV from the IPs (*i.e.* no step to −70 mV first) generated BK currents consistent with the amount of Ca^{2+} likely to have been available at the time of the step up (black traces). Thus, the BK current was larger for the step from the IP of +10 mV than from −30 mV. In both cases, steps to −70 mV even as short as 0.5 msec (red traces) led to the generation of BK currents at +130 mV that were smaller than they were without the step to −70 mV. Evidently, by stepping to −70 mV, many of the BK channels that were open during the IPs closed and were not able to be reopened upon being stepped to +130 mV even though the −70 mV—step would have introduced more Ca^{2+}. Longer durations (greater than 0.5 msec) spent at −70 mV further closed the BK channels leading to a decline in the BK current magnitude measured at +130 mV.

Discussion

BK channels are well positioned to report the Ca^{2+} concentration changes that occur during and after Ca^{2+} entry through Ca^{2+} channels. The spacing of intramembraneous particles thought to be Ca^{2+} and BK channels in freeze-fracture replicas of these active zones (Roberts *et al.,* 1990) suggests that the BK channels are on the order of 10 nm away from Ca^{2+} channels. A more recent report estimated the distance between rat brain Ca^{2+} and BK channels to be ~10–15 nm (Berkefeld *et al.,* 2006). These authors, using affinity purification techniques, showed that BK channels co-isolate into macromolecular complexes with voltage gated Ca^{2+} channels. Further evidence for the close association of BK and Ca^{2+} channels is provided by the finding that millimolar concentrations of the Ca^{2+} chelator BAPTA can intercept the Ca^{2+} entering through voltage-gated channels to prevent BK channel activation while the slower Ca^{2+} buffer EGTA is ineffective (Roberts, et. al., 1990; Prakriya and Lingle, 2000; Berkefeld et al., 2006). These results are consistent with the differential effects of these buffers on transmitter release (Adler et al., 1991; Augustine et. al., 2003) suggesting that BK channels are at a similar distance from the Ca^{2+} channels as are the Ca^{2+} sensors in the release apparatus.

BK channels monitor the rate and duration of Ca^{2+} entry

We find that the rate and duration of Ca^{2+} entry through Ca^{2+} channels are correlated with the time to onset and magnitude of BK currents. The profile of intracellular Ca^{2+} concentration changes near Ca^{2+} channels seems to be what the BK channels report. Rapid but brief rates of Ca^{2+} entry at potentials with large Ca^{2+} driving forces but where Ca^{2+} channels tend to close (*e.g.* −70 mV, Figure 3) yield BK currents with the shortest delay to onset—consistent with locally higher Ca^{2+} concentrations. On the other hand, slower, continuous Ca^{2+} entry at higher potentials (*e.g.* +50 mV, Figure 3) activates more BK channels but only after a longer delay to onset—consistent with a lower concentration of Ca^{2+} reaching a greater number of BK

channels. The maximum BK current measured in response to continued, slow Ca^{2+} influx rates required longer times than were needed with larger Ca^{2+} driving forces.

BK channels deactivate slowly at depolarized levels after exposure to high Ca^{2+}

Our results suggest that the slow decline in the BK current measured at +130 mV following steps to IPs that allow Ca^{2+} influx is either due to the rate of decline of the free Ca^{2+} in the vicinity of the BK channels or is a result of the rate of deactivation of the channels in the absence of an increased Ca^{2+} concentration.

We used two methods to shut off Ca^{2+} entry—by going to E_{Ca} (stepping to +130 mV) or by closing the Ca^{2+} channels (stepping to −70 mV). These two methods have different effects on the BK channels. By stepping to +130 mV the BK channels—while being deprived of continuous Ca^{2+} influx—will still be depolarized. At this potential some channels remain open for tens of msec. Apparently, BK channels are slow to deactivate at depolarized voltages if they have previously been exposed to a high enough Ca^{2+} concentration to open them. This is true even if the ambient Ca^{2+} concentration falls to a level that will not allow them to open *de novo*. This finding supports the conclusions of Cox and Aldrich (2000) that the BK channel's affinity for Ca^{2+} is higher when the channel is open than when it is closed. In our preparation the BK channels may be remaining open for prolonged periods of time after cessation of Ca^{2+} entry at +130 mV because they are binding more tightly the Ca^{2+} that opened them. On the other hand, some of the BK channels that do close at +130 mV can remain sensitive to Ca^{2+} and can re-open if exposed to a high enough $[Ca^{2+}]$ (as can be provided for example by a Ca^{2+} tail current—Figure 4B).

The second method we used to stop Ca^{2+} entry—stepping to −70 mV to close the Ca^{2+} channels—also repolarizes the BK channels. Hair cell BK channels close quickly at −70 mV—the tail current decays exponentially with a time constant of 1.0 ms at −70 mV (Hudspeth and Lewis, 1988). We find that BK channels cannot be reopened upon redepolarization from prolonged stays at −70 mV (Figures 4C and 4D). The implication from this finding is that opening the channels requires a higher concentration of Ca^{2+} than is needed to keep them open. Our results provide an upper limit of ~2.0 msec to the time that the $[Ca^{2+}]$ remains above threshold to open BK channels after the cessation of Ca^{2+} entry. This conclusion stems from the finding that BK currents are unactivatable by a large depolarizing step given 2.0 msec after the peak of a Ca^{2+} tail current (Figures 3 and 4).

The present report demonstrates that the rate of activation and delay to onset of BK channels reflect the dynamic changes in intracellular Ca^{2+} concentration close to Ca^{2+} channels during and after the transient influx of Ca^{2+}.

Acknowledgments

Grants

This work was supported by the National Science Foundation Research in Undergraduate Institutions Grant #0854551 to B. Yazejian and a National Institutes of Health Minority Access to Research Careers Grant (5T34GM008415-18) to the Biology Department at Mount St. Mary's College.

References

Adl1er EM, Augustine GJ, Duffy SN, Charlton MP. Alien intracellular calcium chelators attenuate neurotransmitter release at the squid giant synapse. J Neurosci 1991;11:1496–1507. [PubMed: 1675264]

Armstrong CE, Roberts WM. Electrical properties of frog saccular hair cells: distortion by enzymatic dissociation. Neurosci 1998;18:2962–2973.

Armstrong CE, Roberts WM. Rapidly inactivating and non-inactivating calcium- activated potassium currents in frog saccular hair cells. J Physiol 2001;56:49–65. [PubMed: 11579156]

Augustine GJ, Charlton MP, Smith SJ. Calcium action in synaptic transmitter release. Annu Rev Neurosci 1987;10:633–693. [PubMed: 2436546]

Augustine GJ, Santamaria F, Tanaka K. Local calcium signaling in neurons. Neuron 2003;40:331–346. [PubMed: 14556712]

Berkefeld H, Sailer CA, Bildl W, Rohde V, Thumfart J-O, Eble S, Klugbauer N, Reisinger E, Bischofberger J, Oliver D, Knaus H-G, Shulte U, Fakler B. BK_{Ca}- Cav channel complexes mediate rapid and localized Ca^{2+}-activated K^+ signaling. Science 2006;314:615–620. [PubMed: 17068255]

Bezanilla F, Armstrong CM. Inactivation of the sodium channel. I. Sodium current experiments. J Gen Physiol 1977;70:549–566. [PubMed: 591911]

Clapham DE. Calcium signaling. Cell 2007;131:1047–1058. [PubMed: 18083096]

Cox DH, Aldrich RW. Role of the beta1 subunit in large-conductance Ca^{2+}- activated K^+ channel gating energetics. Mechanisms of enhanced Ca^{2+} sensitivity. J Gen Physiol 2000;116:411–432. [PubMed: 10962017]

Fettiplace R, Fuchs PA. Mechanisms of hair cell tuning. Ann Rev Physiol 1999;61:809–834. [PubMed: 10099711]

Fuchs PA. Time and intensity coding at the hair cell's ribbon synapse. J Physiol 2005;566.1:7–12. [PubMed: 15845587]

Glowatzki E, Fuchs PA. Transmitter release at the hair cell ribbon synapse. Nat Neurosci 2002;5:147–154. [PubMed: 11802170]

Horn R, Marty A. Muscarinic activation of ionic currents measured by a new whole-cell recording method. J Gen Physiol 1988;92:145–159. [PubMed: 2459299]

Hudspeth AJ, Lewis RS. Kinetic analysis of voltage- and ion-dependent conductances in saccular hair cells of the bull-frog, Rana catesbeiana. J Physiol 1988;400:237–274. [PubMed: 2458454]

Issa N, Hudspeth AJ. Clustering of Ca^{2+} channels and Ca^{2+}-activated K^+ channels at fluorescently labeled presynaptic active zones of hair cells. Proc Natl Acad Sci USA 1994;91:7578–7582. [PubMed: 8052623]

Issa N, Hudspeth AJ. The entry and clearance of Ca^{2+} at individual presynaptic active zones of hair cells from the bullfrog's sacculus. Proc Natl Acad Sci USA 1996;93:9527–9532. [PubMed: 8790364]

Katz, B. The release of neural transmitter substances. Liverpool University Press; 1969.

Neher E. Vesicle pools and Ca^{2+} microdomains: new tools for understanding their roles in neurotransmitter release. Neuron 1998;20:389–399. [PubMed: 9539117]

Prakriya M, Lingle CJ. Activation of BK channels in rat chromaffin cells requires summation of Ca^{2+} influx from multiple Ca^{2+} channels. J Neurophysiol 2000;84:1123–1135. [PubMed: 10979988]

Rae J, Cooper K, Gates P, Watsky M. Low access resistance perforated patch recordings using amphotericin B. J Neurosci Methods 1991;37:15–26. [PubMed: 2072734]

Roberts WM. Spatial calcium buffering in saccular hair cells. Nature 1993;363:74–76. [PubMed: 8479539]

Roberts WM. Localization of calcium signals by a mobile calcium buffer in frog saccular hair cells. J Neurosci 1994;14:3246–3262. [PubMed: 8182469]

Roberts WM, Jacobs RA, Hudspeth AJ. Colocalization of ion channels involved in frequency selectivity and synaptic transmission at presynaptic active zones of hair cells. J Neurosci 1990;10:3664–3684. [PubMed: 1700083]

Rutherford MA, Roberts WM. Spikes and membrane potential oscillations in hair cells generate periodic afferent activity in the frog sacculus. J Neurosci 2009;29:10025–10037. [PubMed: 19675236]

Sanchez M, McManus OB. Paxilline inhibition of the alpha-subunit of the high- conductance calcium-activated potassium channel. Neuropharmacol 1996;35:963–968.

Smotherman MS, Narins PM. The electrical properties of auditory hair cells in the frog amphibian papilla. J Neurosci 1999;19:5275–5292. [PubMed: 10377339]

Tucker TR, Fettiplace R. Monitoring calcium in turtle hair cells with a calcium- activated potassium channel. J Physiol 1996;494:613–626. [PubMed: 8865061]

Yazejian B, Sun XP, Grinnell AD. Tracking presynaptic Ca^{2+} dynamics during neurotransmitter release with Ca^{2+}-activated K^+ channels. Nat Neurosci 2000;3:566–571. [PubMed: 10816312]

Zucker RS. Exocytosis: a molecular and physiological perspective. Neuron 1996;17:1049–1055. [PubMed: 8982154]

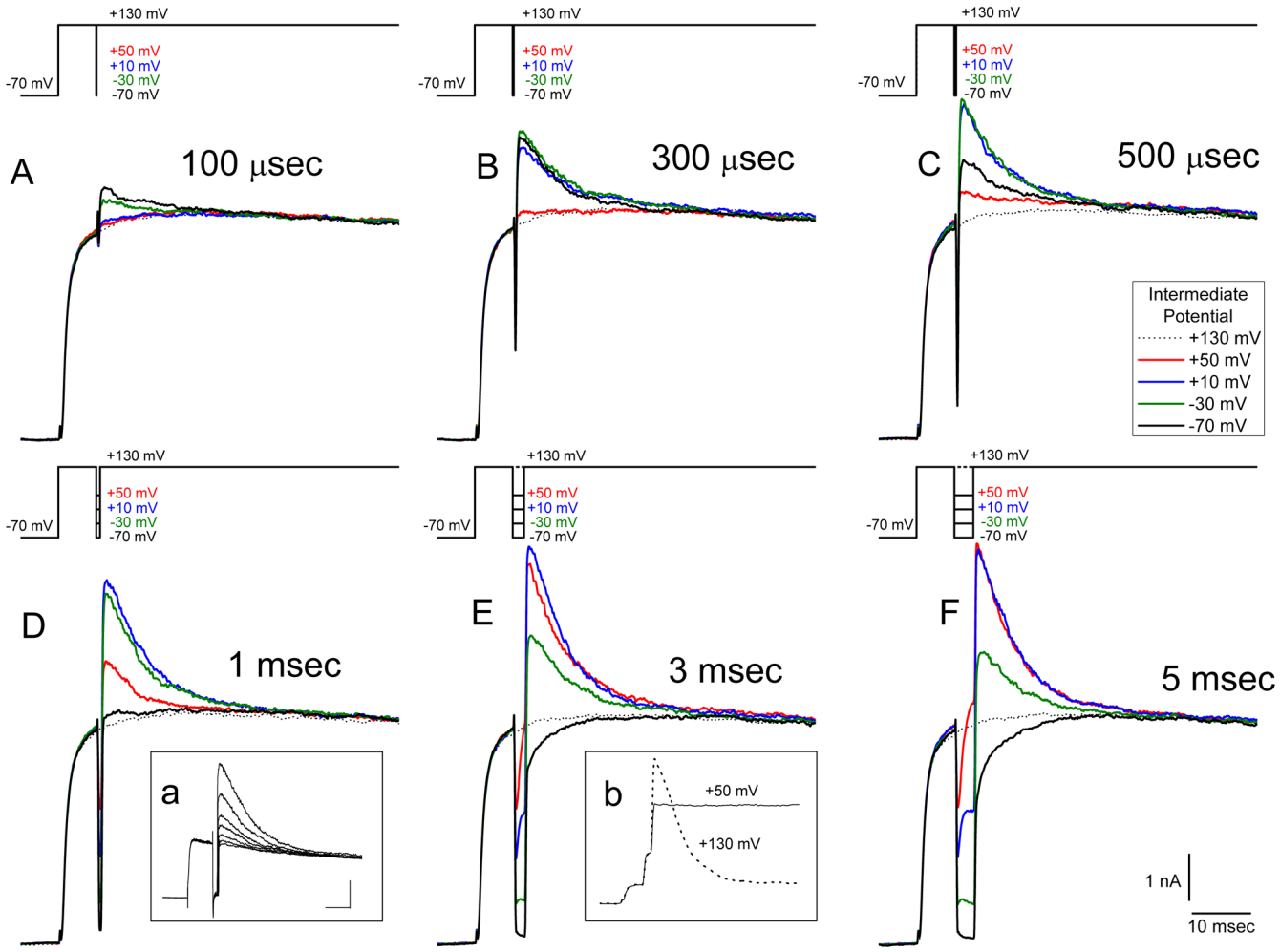

Figure 1.

BK currents activated in response to different rates and durations of Ca^{2+} influx. Current records in this and all figures are the average of three presentations of the voltage waveform. Stimulus waveforms are given above each set of traces—most clearly delineated in F. In all records the membrane potential was first stepped from a holding potential of −70 mV to +130 mV for 5 msec to open Ca^{2+} channels but not allow Ca^{2+} entry. The potential was then transiently stepped to intermediate potentials of +50 mV, +10 mV, −30 mV or −70 mV for 100 µsec, 300 µsec, 500 µsec, 1 msec, 3 msec or 5 msec to allow Ca^{2+} entry before re-depolarization to +130 mV to stop Ca^{2+} influx. A-F: Current responses to various times and intermediate potential voltages. The dotted line in each record shows the response to a step to +130 mV only (*i.e.* no intermediate voltage step). Inset a shows—in a different cell—the progressive block of BK current in response to application of 100 nM paxilline. Voltage presentations were given at 5 sec intervals: IP was −50 mV, 3 msec; scale bars 2 nA, 10 msec. Inset b—also from a different cell—shows the current responses to test pulses of +130 mV (dotted line) and +50 mV (solid line) after IP steps to +10 mV. Scale bars are the same as in inset a.

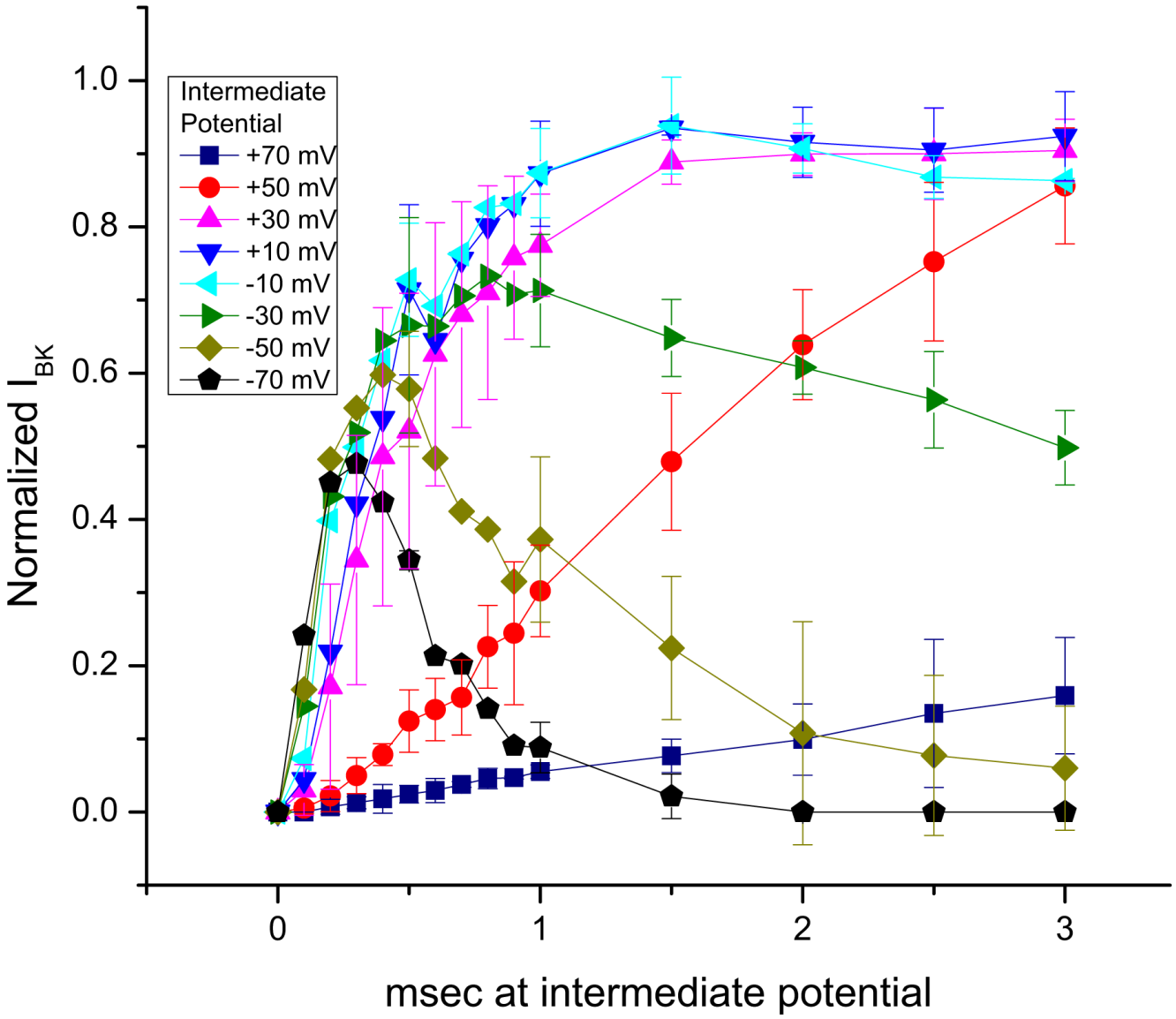

Figure 2.
Summary data of normalized peak BK current measured at +130 mV vs. time spent at each of the intermediate potentials. Each symbol represents an average of six experiments like that of Figure 1. Error bars represent ±SD.

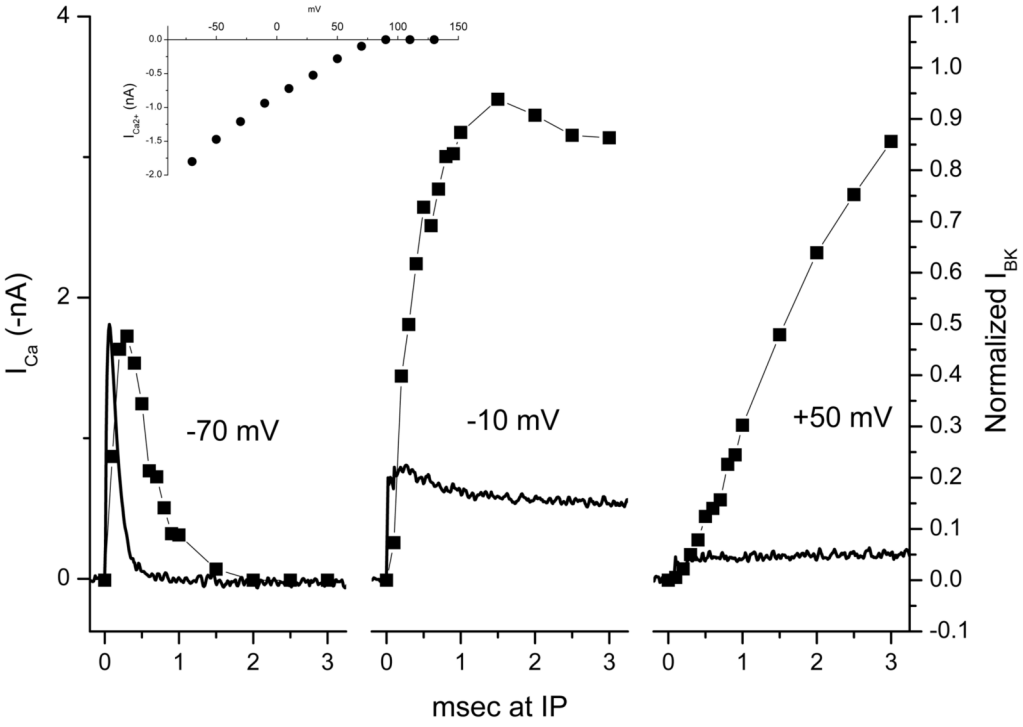

Figure 3.

Correlation of BK current magnitude measured at +130 mV with Ca^{2+} influx at three intermediate potentials. Continuous traces are Ca^{2+} currents (inverted for clarity) measured at the indicated potentials after a step from +130 mV (voltage steps not shown). Symbols are average peak normalized BK currents measured at +130 mV (taken from Figure 2) after different durations at the IPs. Ca^{2+} currents and BK currents were measured in different cells. The inset shows the relationship between the Ca^{2+} current and voltage for steps from +130 mV.

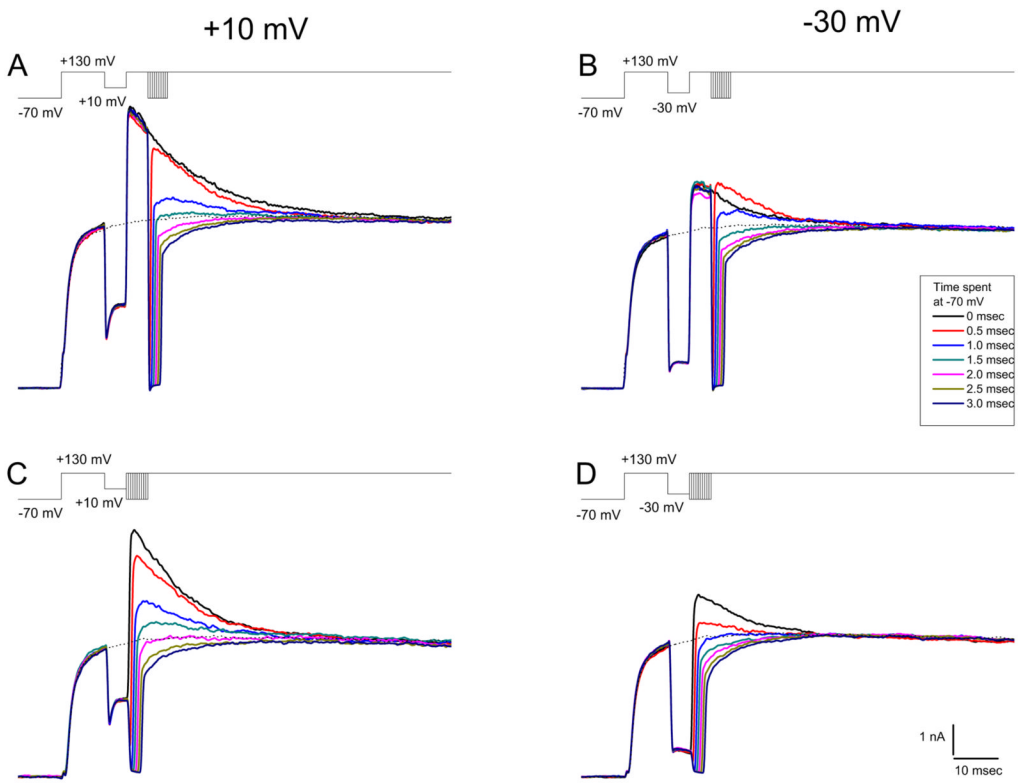

Figure 4.

Deactivation of BK currents. Stimulus waveforms are presented above each set of currents records. In A and B, a step to +130 mV was followed with an intermediate step to +10 and −30 mV respectively followed by a second depolarization to +130 mV (as in Figure 1). The second +130 mV step was interrupted after 5 msec by steps to −70 mV for 0 msec (*i.e.* no step to −70 mV), 0.5 msec, 1.0 msec, 1.5 msec, 2.0 msec, 2.5 msec, or 3.0 msec before a third depolarization to +130 mV. In C and D, after an intermediate step to +10 mV and −30 mV respectively, a second depolarization to +130 mV was given except that it was *preceded* by steps to −70 mV for the same times as in A and B. For all records the dotted line represents the current response to a step to +130 mV only.